

Study of the structure and kinematics of the NGC 7465/64/63 triplet galaxies

O.A. Merkulova^{1,a}, G.M. Karataeva^a, V.A. Yakovleva^a, A.N. Burenkov^b

^aAstronomical Institute of Saint-Petersburg State University

^bSpecial Astrophysical Observatory, Russian Academy of Sciences

Abstract

This paper is devoted to the analysis of new observational data for the group of galaxies NGC 7465/64/63, which were obtained at the 6-m telescope of the Special Astrophysical Observatory of the Russian Academy of Sciences (SAO RAS) with the multimode instrument SCORPIO and the Multi Pupil Fiber Spectrograph. For one of group members (NGC 7465) the presence of a polar ring was suspected. Large-scale brightness distributions, velocity and velocity dispersion fields of the ionized gas for all three galaxies as well as line-of-sight velocity curves on the basis of emission and absorption lines and a stellar velocity field in the central region for NGC 7465 were constructed. As a result of the analysis of the obtained information, we revealed an inner stellar disk ($r \approx 0.5$ kpc) and a warped gaseous disk in addition to the main stellar disk, in NGC 7465. On the basis of the joint study of photometric and spectral data it was ascertained that NGC 7464 is the irregular galaxy of the IrrI type, whose structural and kinematic peculiarities resulted most likely from the gravitational interaction with NGC 7465. The velocity field of the ionized gas of NGC 7463 turned out typical for spiral galaxies with a bar, and the bending of outer parts of its disk could arise owing to the close encounter with one of galaxies of the environment.

Key words: galaxies, groups of galaxies, interacting galaxies – kinematics, structure

1 Introduction

The NGC 7465/64/63 triplet belongs to the NGC 7448 group that consists of 9 galaxies with line-of-sight velocities from 1800 to 2350 km/s and with the velocity variance of ~ 150 km/s (Li and Seaquist, 1994). A summary of main properties of the NGC 7465/64/63 galaxies (which were taken from other papers and obtained during our study) is given in Table 1. Both individual galaxies and the whole group have been studied intensively. The extensive

¹E-mail: olga_merkulova@list.ru

Table 1: Main characteristics of the NGC 7465/64/63 galaxies

Characteristics	NGC 7465	Refer.	NGC 7464	Refer.	NGC 7463	Refer.
Morphological type	(R')SB0 ⁰	RC3	E1 pec	RC3	SABb: pec	RC3
	Sab?	1	IrrI	1		
V_{hel} , km/s	1963 ± 3	1	1765 ± 2	1	2366 ± 3	1
$B_{t,0}$, mag	13.05	1	14.23	1	12.35	RC3
(B-V) ₀ , mag	0.85	1	0.40	1	0.28	RC3
(V-R) ₀ , mag	0.47	1	0.32	1		
M_B , mag	-19.30	1	-18.12	1	-19.90	LEDA
$F_{H\alpha}^*$, erg/s/cm ²	1.1×10^{-12}	1				
SFR _{Hα} , M_{\odot} /year	0.9	1				
V_{max} , km/s	105	1	40	1	115	1
V_{hel} (HI data), km/s	1962 ± 6	LEDA	1870 ± 9	LEDA	2445 ± 8	LEDA
$F_{\lambda 21cm}$, mag	14.53 ± 0.16	LEDA	14.66 ± 0.15	LEDA	15.33 ± 0.16	LEDA
$\log \frac{M_{HI}}{M_{\odot}}$	$9.70 \pm <0.01$	2	9.3	3	9.2	3
W_{50} , km/s	81	3	292	4	218	4

1 – this paper, 2 – Fernandez et al. (2010), 3 – van Driel et al. (1992), 4 – Springob et al. (2005)

* $F_{H\alpha}$ is the total flux within the 9.3×10^{-19} erg/s/cm²/arcsec² isophote, SFR_{H α} is the corresponding star formation rate.

investigation of six members of the NGC 7448 group in the optical, far infrared and radio ranges (van Driel et al., 1992) showed that most of these galaxies are peculiar. The undisturbed HI distribution and kinematics were revealed in NGC 7448, NGC 7463, UGC 12313, and UGC 12321. In optical images of NGC 7448 and NGC 7463, distortions of outer spiral arms are seen well; NGC 7464 и NGC 7465 have been identified as merger candidates because of their large ultraviolet (UV) excesses, the intense star formation regions, etc. In the optical range, all objects show emission lines; most of the galaxies have HII-type spectra indicating the active star formation; some galaxies rather resemble LINERs. The nuclear activity is observed only in the NGC 7465 galaxy. NGC 7465 together with NGC 7464 and NGC 7463 form a close subgroup.

NGC 7464 and NGC 7465 (Mrk 313) are early-type galaxies with the projected distance between them of 1'.9, and NGC 7463 is classified as a peculiar barred spiral galaxy seen almost edge-on. It is $\sim 0'.7$ distant from NGC 7464 and 2'.5 distant from NGC 7465. These three galaxies have been classified as UV-excess galaxies (Takase, 1980). NGC 7465 was included

in the catalog of Whitmore et al. (1990) in the D category (D-42) — the category of systems possibly related to polar-ring galaxies (PRGs) — because of a faint outer ring at a position angle of $\approx 45^\circ$ that is seen in the optical range.

High resolution 21-cm observations of this compact triplet and another two faint galaxies (UGC 12313 and UGC 12321) from the NGC 7448 group (sometimes these 5 galaxies are united into the small NGC 7465 group) were obtained by Li and Seaquist (1994). It was shown in their paper that tidal disturbances in the HI morphology and kinematics are observed in four of five members of the NGC 7465 group. It was ascertained that an HI “bridge” connects, in projection, UGC 12313 with NGC 7463 or with the triplet as a whole; and sides of both galaxies connected by the “bridge” show signs of the recent interaction. Near the center of NGC 7463, the change in the position angle of the HI disk is observed, and in the same region the velocity field reverses its sign. These peculiarities are explained by the existence of the “high-velocity” gas, most of which is above the eastern side of the galaxy’s optical disk. The HI emission of NGC 7463 is separated from that of NGC 7465/64 in the velocity space. To the south and southeast of NGC 7465 at a distance of $\sim 80''$ (11.4 kpc), an arc-like structure is observed. Together with some weak emission to the north of NGC 7465, they form a ring. Taking into account the orientation of NGC 7465 and the HI ring, authors of the mentioned work suggest that it represents a polar ring around NGC 7465 and could be material pulled out from NGC 7464 during a close encounter with NGC 7465. The southern part of the ring that contains most of the HI flux coincides with the string of condensations seen in optical images at a level of ~ 24 mag arcsec $^{-2}$ in the V band (Casini and Heidmann, 1978; van Driel et al., 1992). However, the optical string apparently extends further to the southwest rather than bends toward NGC 7464, as the HI ring does. Therefore, it is not clear if the optical string and the HI ring are related.

Since the panoramic (2D) spectroscopy makes it possible to obtain a more complete kinematical picture of an object, especially in the case of the presence of several components, the peculiar galaxies NGC 7465/64/63 were included in the program of our investigation. This paper is the continuation of the study of candidates for PRG by the 2D-spectroscopy methods that was started in the paper of Shalyapina et al. (2007). In addition to spectral observations, we tried to obtain deep images in the optical range for a more detailed study of the morphology and structure of these objects. In the next section the brief information about instruments used for observations and about methods of the data processing is given. Then the results of our study of the structure and kinematics of each galaxy are presented. In conclusion the discussion of all available data is carried out.

As distances to the NGC 7465/64/63 galaxies, we take the distance to the NGC 7448 group of 29.5 Mpc ($H_0 = 75$ km/s/Mpc) (van Driel et al., 1992); then a scale is: $1'' = 0.14$ kpc.

2 Observations and processing

Observations of the NGC 7465/64/63 galaxies were performed at the 6-m telescope of SAO RAS. The detector was the EEV 42-40 CCD-array of 2048×2048 pixels (each pixel size is $13.5 \times 13.5 \mu m$).

Photometric observations of the galaxies in the Johnson B and V bands and in the Cousins R band were performed using the SCORPIO focal reducer (Afanasiev and Moiseev, 2005) at the night of 16 to 17 August, 2004. For the calibration, standard stars from a list of Landolt (1983) were observed during the night. The information about the photometric observations is given in Table 2. The observations were processed using the ESO-MIDAS software package.

Table 2: Photometric observations

Object	Band	Exposure time (frames \times s)	z, deg
NGC 7465/64/63	B	$600 + 2 \times 300 + 2 \times 30$	40–44
	V	9×60	37–40
	R_c	$4 \times 30 + 2 \times 20 + 3 \times 120$	35–37

Transparency coefficient values average for SAO RAS (Neizvestnyi, 1983) were used in the reduction for the atmosphere. An accuracy of total magnitude estimates of galaxies is $\pm 0^m.1$.

Spectral observations of the galaxies were also carried out at the prime focus of the 6-m telescope, using the SCORPIO focal reducer in modes of the Interferometer Fabry-Perot (IFP) or of the long-slit spectroscopy (LS) and using the Multi Pupil Field Spectrograph (MPFS) (see the SAO RAS web site², Afanasiev et al., 2001). A log of observations of the galaxies is given in Table 3.

Parameters of the focal reducer during the interferometric observations are given in Moiseev (2002). The preliminary monochromatization was carried out using the narrow-band filter IFP 661 with a central wavelength λ_c of 6604 \AA and a full width at half maximum $\text{FWHM} = 21 \text{ \AA}$. The spacing between adjacent orders of interference was 28 \AA (1270 km/s). The spectral resolution of the IFP was 2.5 \AA ($\approx 110 \text{ km/s}$). The readout of the detector (EEV 42-40 CCD-array) was carried out in the mode of 4×4 pixel hardware averaging, so 512×512 pixel images (the pixel size was $0.714''$) were obtained in each spectral channel.

The processing of interferometric observations was carried out using the software developed at SAO RAS (Moiseev, 2002). After primary procedures (the subtraction of night-sky lines and the reduction to the wavelength scale), the observational data represented “data cubes”, where

²http://www.sao.ru/hq/lsvfo/devices/mpfs/mpfs_main.html

Table 3: Spectral observations

Object	Instrument, data	Exposure time, s	Field	Seeing, arcsec	Spectral region, Å	P.A.
NGC 7465	LS 16.08.2006	4×1200	1'' × 6'	1.8	4800–5570	160°
NGC 7465/64/63	IFP 16.08.2006	32×180	6' × 6'	1.8	H α	
NGC 7465	LS 26.07.2008	2×900	1'' × 6'	1.6	5700–7400	161°
NGC 7465	LS 27.07.2008	2×1200	1'' × 6'	2.9	5700–7400	45°
NGC 7465	MPFS 05.08.2008	3×900	16'' × 16''	2.0	4196–5712	Central region
NGC 7465	MPFS 08.08.2008	4×900	16'' × 16''	3.0	5630–7166	Central region

each point in a 512×512 -element field contained a 32-channel spectrum. The optimal data filtering — a Gaussian smoothing over spectral coordinate with FWHM equal to 1.5 channels and the two-dimensional Gaussian smoothing over spatial coordinates with FWHM = 2 pixels — was carried out. The Gaussian fitting of the H α and [NII] $\lambda 6584$ Å emission line profiles was used to construct velocity fields and monochromatic images. Measurement errors of line-of-sight velocities for lines with symmetric profiles were about 10 km/s. We also constructed images in the 6592.0–6619.35 Å (near H α) continuum.

For the analysis of a velocity field we used the “tilted-ring” method (Begeman, 1989; Moiseev, Mustsevoi, 2000); it makes it possible to determine a dynamical center position and a position angle of dynamical axis, to refine an inclination of a galaxy to the plane of the sky, and to construct a rotation curve. The analysis of the dependence of the positional angle of dynamical axis and of the inclination on radius gives the information about features of the gas motion in the galaxy.

The long-slit observations of NGC 7465 were performed in two spectral ranges: “green” and “red”. In the “green” range containing the H β , [OIII] $\lambda\lambda 4959, 5007$ Å emission lines and the absorption lines of the old stellar population MgI 5175Å, FeI + Ca 5270 Å and others, we used the VPHG2300G grism with the spectral resolution $\delta\lambda = 2.2$ Å in the range $\Delta\lambda = 4800$ –5570Å. The VPHG1200R grism was used for the “red” range $\Delta\lambda = 5700$ –7400Å (the vicinity of the H α line), and the spectral resolution was equal to 5 Å. The processing of the obtained data was performed using standard procedures of the ESO-MIDAS package. After the primary reduction, the smoothing along the slit with a rectangular window 3 pixel in height was carried out to increase the signal-to-noise ratio. Line-of-sight velocities of the gaseous component

were measured from positions of centers of Gaussians fitted to emission lines. An accuracy of these measurements was estimated by the night-sky HgI $\lambda 5461 \text{ \AA}$ and [OI] $\lambda 6300 \text{ \AA}$ lines and was $10\text{-}15 \text{ km s}^{-1}$. The cross-correlation method (Tonry, Davis, 1979) was used to determine line-of-sight velocities and velocity dispersions from absorption lines.

MPFS simultaneously takes spectra from 256 spatial elements (in the form of square lenses) that form a 16×16 -element array in the plane of the sky. During our observations, the angular size of one element was $1''$. The spectral resolution was 3 \AA . The comparison spectrum of the He-Ne-Ar lamp was used for the wavelength scale calibration; the linearization accuracy was $\sim 0.3 \text{ \AA}$. The processing of the MPFS spectra was carried out using a software package developed by V.L. Afanasiev and A.V. Moiseev (SAO RAS).

3 Multicolor photometry

During photometric observations, the task was to reveal faint tidal structures between the galaxies of the triplet and to study the expected polar ring, so a frame was centered on NGC 7465, and the most distant galaxy NGC 7463 is not whole in the frame. The image of NGC 7465/64/63 in the B band with the superimposed isophotes in the $H\alpha$ line and the isophotes in the B , V , R_c bands are presented in Fig. 1. We obtained deeper images than in earlier works (van Driel et al., 1992; Schmitt, Kinney, 2000), and in our images the features of outer regions of galaxies are seen more clearly.

Despite the ragged structure of the NGC 7465 galaxy, three spiral arms and not a faint ring, the presence of which was pointed out earlier by several authors (see, e.g., van Driel et al., 1992, etc.), are prominent. The northeastern and southeastern arms are superimposed on the arc-like structure observed in HI and called the polar ring by Li and Seaquist (1994). The southwestern arm bends and extends to the northwest in the direction of the NGC 7464 galaxy, whose isophotes are asymmetric and stretched in the direction of this arm. Three spirals manifest themselves in the color index distribution too (Fig. 1). However, only the brightest parts of the spirals that are close to the main body of the galaxy are seen because of the ragged structure and the low surface brightness at the ends of spirals.

As noted above, NGC 7463 is not whole in the frame, but in its images a central bar-like structure and an eastern spiral arm, whose end turns to the north, are clearly seen.

The total apparent magnitudes in three bands and the integrated color indices of NGC 7465 and NGC 7464 were obtained using the multiaperture photometry method, whose accuracy (as it was mentioned above) was $\pm 0^m.1$. But emission lines find themselves within the bandwidth of all three filters, and this can lead to the increase of errors, especially in regions where the contribution of the radiation in emission lines is considerable. The total magnitudes corrected

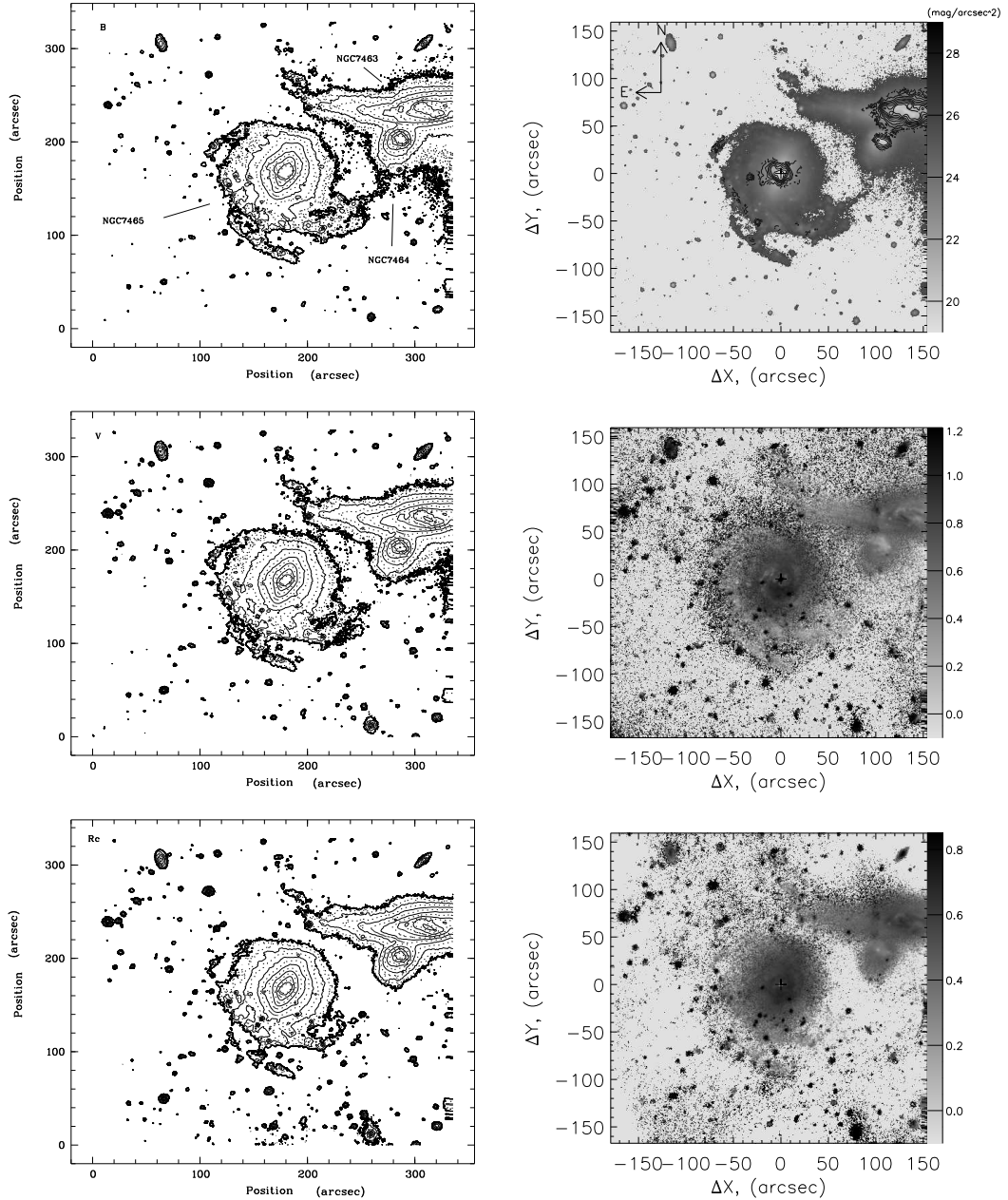


Figure 1: Left column top-down: isophotes of the galaxies in the B , V , R_c bands (with a step equal to $0.5 \text{ mag}/\square''$; the most outer isophote in the B band corresponds to the surface brightness of 26 mag , that in V corresponds to 25.5 mag , and that in R_c corresponds to 25 mag). Right column top-down: the image in the B band with the superimposed isophotes in the $H\alpha$ line, $B-V$ and $V-R_c$ color distribution maps.

for the extinction in our Galaxy (Schlegel et al., 1998) are given in Table 1. Color indices of NGC 7464 are close to values typical for IrrI galaxies, and color indices of NGC 7465 are close to values typical for Sa-Sab galaxies.

The $B-V$ и $V-R_c$ color distributions are presented in Fig. 1. As follows from these maps, the bluest color indices are observed in the circumnuclear region of NGC 7464 ($B-V \approx 0^m2$) and

in the region of spiral arms of NGC 7465 ($\approx 0^m.36$) and NGC 7464 ($\approx 0^m.3$). In the circumnuclear region of NGC 7465, values of color indices are distorted due to presence of emission lines. At a distance of from $10''$ to $30''$ from the nucleus, $B-V$ changes little ($0^m.7-0^m.8$); then it gradually turns blue and reaches $0^m.36$ in the region of spiral arms. The color index distribution in the main body of NGC 7463 is extremely nonuniform which seems to be connected with the presence of the bar, numerous HII-regions, and the dust lane, where $B-V$ is $\approx 0^m.8$.

4 Morphology and structure of the triplet galaxies

For the analysis of the photometric structure of the galaxies, we used a technique proposed by Jedrzejewsky (1987). It is based on the Fourier expansion of the deviation of isophotes from the elliptic shape. For this purpose, the IRAF system was used for the data processing. Let us consider results for each galaxy that were obtained by us.

NGC 7465. In the central region ($r \leq 5''$), isophotes in the R_c band have approximately elliptic shape with the ellipticity $\epsilon \approx 0.2$ and the position angle of the major axis $PA \approx 120^\circ$. We also analyzed the shape of isophotes in this region in “red” and “green” continua from the IFP and MPFS data (Fig. 2), in order to eliminate the influence of emission lines. It turned out that values of both ϵ and PA coincide with corresponding values of the broadband photometry.

Images in the circumnuclear region of the galaxy in continua (F547M and F791M filters) were obtained with the wide-field camera (WFPC2) of the Hubble Space Telescope (HST) (Ferruit et al., 2000). Thanks to the high spatial resolution (of the order of $0.1''$), a series of interesting details manifest itself in these images. Figure 2 presents a HST frame in the F547M filter. Regions brightest in the continuum are located within a circle with $r = 4''$ and display an inverted S -shaped morphology with the position angle of the major axis $PA \approx 120^\circ$; then the major axis turns gradually, and $PA \approx 160^\circ - 165^\circ$ at a distance of $10''$. The morphology of central regions to the southeast of the nucleus is distorted strongly by dust lanes perpendicular to the major axis of the galaxy. A deep compact minimum in the $\log(F547M/F791M)_{ratio} (\simeq -0.15)$ suggestive of the strong reddening corresponds to the nucleus.

According to our data (both the continuum and broadband observations), ϵ increases with the increase of the distance from the center of the galaxy from 0.2 ($r = 2''$) to ~ 0.35 (at $r = 10'' - 30''$) and decreases gradually to 0.2 in the region of spiral arms; PA increases from 120° to 160° at r from $2''$ to $\sim 15''$ and is constant further. Such behavior of PA agrees with the HST data and with earlier ground-based observations in the continuum (van Driel et al., 1992; Mulchaey et al., 1996). The change of ellipticity in outer ($r > 30''$) parts of the galaxy is probably connected with the violation of the symmetry of spiral arms relative to the center owing to the interaction.

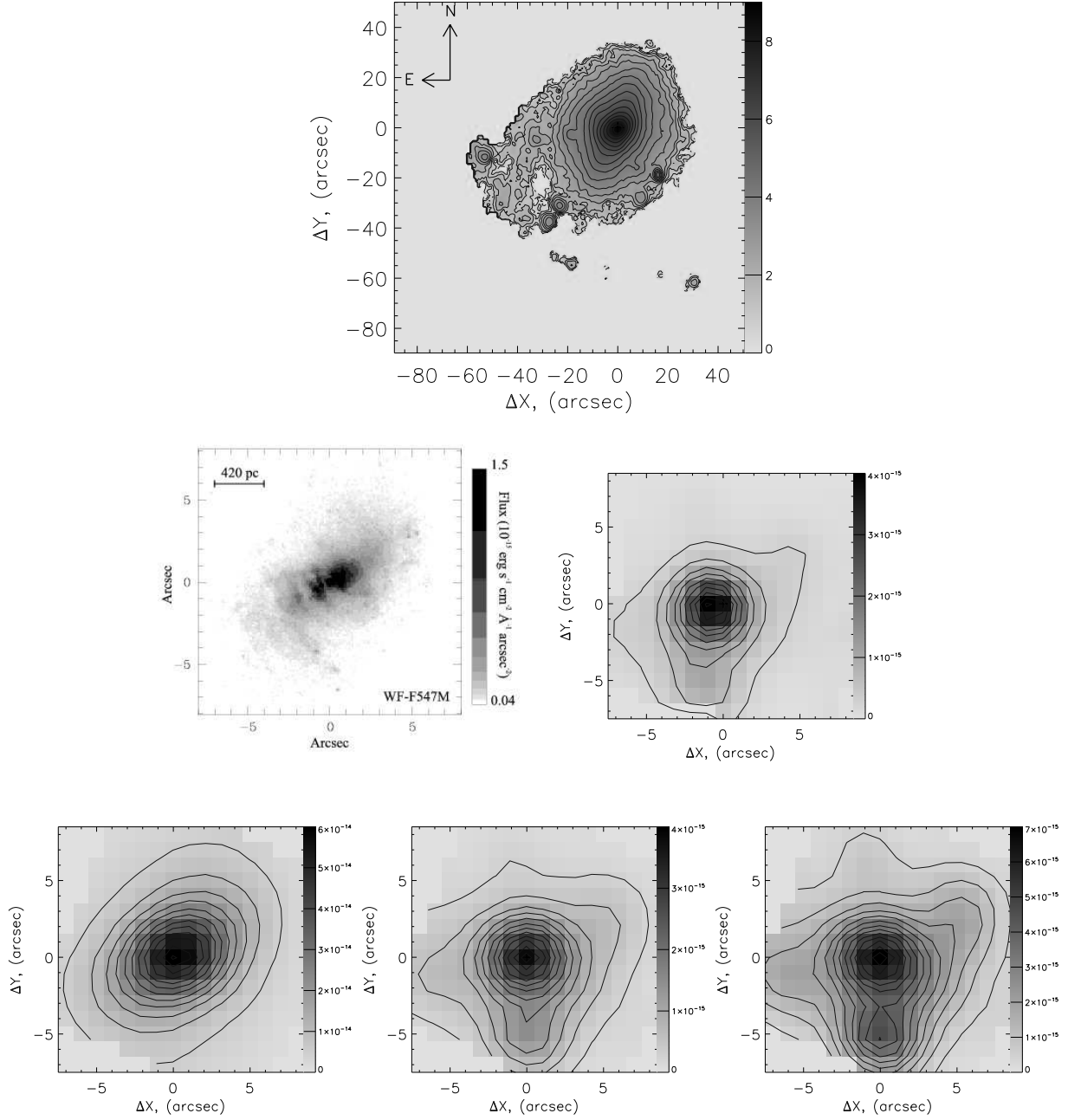


Figure 2: NGC 7465. Top: the image in the continuum near $H\alpha$ according to the IFP data. Middle: left: the image in the continuum in the F547 filter (Fig. 24 (top, right) from Ferruit et al. (2000)); right: the image in the [OIII] λ 5007 \AA line according to the MPFS data. Bottom from left to right: images in the continuum near $H\alpha$, in the [NII] λ 6584 \AA line, and in the $H\alpha$ line according to the MPFS data.

We also carried out the analysis of the photometric structure of NGC 7465 in the K_s band, using data of the Two Micron All Sky Survey (2MASS). The galaxy disk radius in the image in this band is $\approx 23''$. In the central region $PA \approx 120^\circ$; with the distance from the center, PA increases up to 160° (at $r = 15''$) and then it remains approximately constant. The ellipticity

changes from 0.2 to ≈ 0.4 , and this coincides with the behavior of these parameters in the optical range.

The brightness distribution of NGC 7465 in the R_c band was used for the decomposition into components. Two regions can be singled out in the profile along $PA = 160^\circ$: the central one (up to $r \approx 5'' - 7''$ from the center) with a steeper shape of the profile and an extended outer one ($7'' \leq r \leq 40''$) where the profile is less steep. The brightness profile in the outer region is well represented by the exponential law with a scale factor $h_d = 7''.4$ and a central surface brightness $\mu_d = 18^m0$, along the almost whole length. After the subtraction of an exponential disk with the values of h_d and μ_d that were found above, at $PA = 160^\circ$ and $i = 50^\circ$ taken from the observed brightness distribution, the central structure stretched in the direction of 120° is seen more clearly. We tried to approximate the photometric cut along this direction by the Sersic law. The best agreement with the observed profile is reached at the following parameters: the index $n = 1 \pm 0.2$ (such index is typical for disks), the effective radius $R_{e,b} = 4''.6$, and the central surface brightness $\mu_b = 16^m3$.

Let us proceed to the analysis of the brightness distribution in emission lines. The comparison of brightness distributions in the continuum and in $H\alpha$ (Fig. 2 and 1) showed that they differ noticeably. Isophotes in $H\alpha$ are stretched along the NE-SW direction ($PA \sim 50^\circ$), and their shape is far from elliptic one (according to a rough estimation, $\epsilon \sim 0.3$ ($i \sim 46^\circ$)). The radiation maximum corresponds to the galaxy nucleus, and a slightly less bright region is south of the nucleus at $r \approx 5''$; other less bright condensations are also observed. On the SE side, an arched outgrowth with the brightening at its end which apparently relates to the SE spiral arm is well noticeable. A string of regions lighting in the $H\alpha$ line is singled out on the southeast side at a distance of $55'' - 70''$ from the galaxy center. This string looks like a ‘‘ragged’’ semiring. One more, extended region bright in $H\alpha$ is seen to NE at a distance of $\sim 80''$ from the center. Let us note that all these regions fall on spiral arms of the galaxy. A total flux in the $H\alpha$ line and a lower estimate of the star formation rate (with no account taken of the extinction) that was obtained on the basis of the relation from Kennicutt (1998) are given in Table 1.

The comparison of brightness distributions in the permitted ($H\alpha$, $H\beta$) and forbidden ([NII], [SII], [OIII]) emission lines (Fig. 2) for the central region of the galaxy shows that images in all emission lines are similar and there are no considerable differences in the extent of the emission.

NGC 7464. The brightness distribution both in broadband filters and in the continuum (Fig. 1, 3) is amorphous, and the shape of isophotes is approximately elliptic. In the central region ($r \leq 7''$), $PA \sim 50^\circ$ and the ellipticity changes from 0.3 ($r \approx 2''$) to 0.1 ($r \approx 8''$). At a distance of $\approx 9'' - 11''$, isophotes are round, then ϵ increases up to 0.2 ($r \approx 15''$); PA in outer parts is $\sim 120^\circ$. The photometric profile along the major axis ($PA = 120^\circ$) is asymmetric; the SE-wing is flatter. The stretching in the direction of the SW spiral arm of NGC 7465 increases

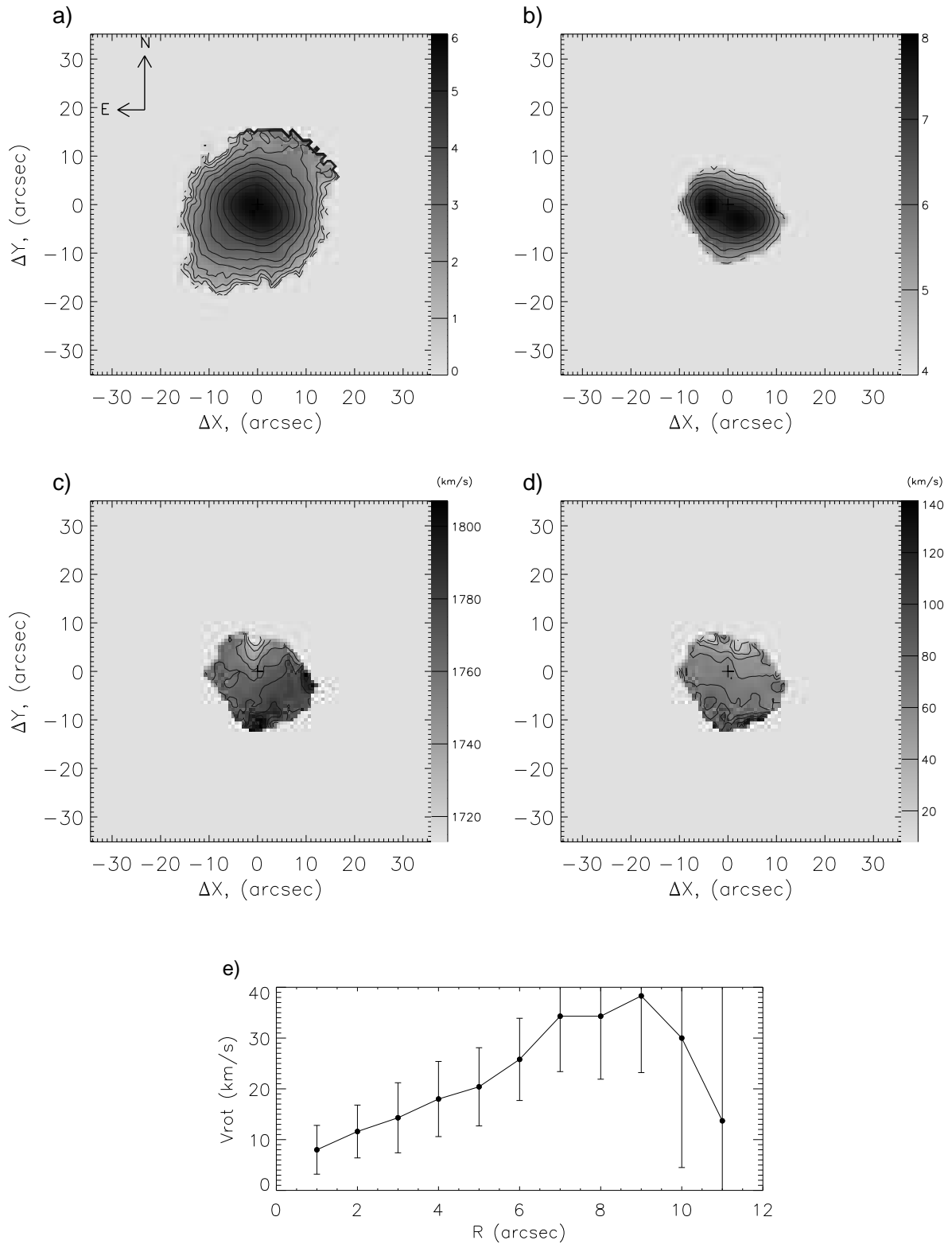


Figure 3: NGC 7464. Results from the IFP data: (a) — the brightness distribution in the narrow continuum near the H α line; (b) — the brightness distribution in the H α line; (c) — the line-of-sight velocity field in the H α line; (d) — the line-of-sight velocity dispersion field in the H α line. Results of the “tilted-ring” method: (e) — the rotation curve of the gas.

with the distance from the center, as we have already mentioned in the section “Multicolor Photometry”. The turn of PA from $\approx 50^\circ$ in the center to $\approx 120^\circ$ in outer parts is observed.

Brightness distributions in the $H\alpha$ and $[NII] \lambda 6584 \text{ \AA}$ lines are similar, therefore in Fig. 3 we give only the image in the $H\alpha$. In the central part, two bright regions located approximately along the direction of 65° on both sides from the nucleus and embedded in to the diffuse radiation in these lines are prominent. It was noted in van Driel et al. (1992) that there is possibly a bar in the center of this galaxy; but our study of the kinematics (see the following section) does not confirm the presence of the bar. PA of outer isophotes ($r \geq 8''$) is $\approx 68^\circ$. We should note that isophotes in emission lines are turned relative to isophotes in the continuum.

NGC 7463. Figures 1 and 4a present brightness distributions in broadband filters and the continuum, respectively. Main parameters of the bar are: $PA_{\text{bar}} \approx 57^\circ$, the ellipticity of bar is $\epsilon_{\text{bar}} \approx 0.7$, and the size of the semimajor axis of bar a_{bar} is $\approx 11''$. The disk of the galaxy has the following characteristics: $PA_{\text{disk}} \approx 90^\circ$, and ϵ_{disk} changes smoothly from 0.45 at a distance of $12''$ to 0.6 at $r = 30''$ (the inclination of the disk changes from 57° to 66°). Outer parts of the disk are asymmetric relative to the minor axis; the western part looks more disturbed, and the turn/bend of this part of the disk to the south is observed.

In the image of the galaxy in the $H\alpha$ line (Fig. 4b), the bar-like structure is not singled out, but only two brightenings at its ends are seen, and the brightness of the eastern one is higher. In addition, several bright condensations located along spiral arms are observed in the given image, and they are probably HII-regions. All this is embedded into the diffuse radiation in the $H\alpha$ line that extends approximately to the same distances as the radiation in the continuum.

5 Kinematics of gas and stars

Spectral observations of the triplet galaxies included observations with IFP. On their basis, line-of-sight velocity fields and velocity dispersion maps in the $H\alpha$ line for each of galaxies (Fig. 5, 3c,d, 4c,d) as well as in the $[NII] \lambda 6584 \text{ \AA}$ line for NGC 7464 were constructed. For NGC 7465, the more detailed spectral study was performed (see Table 3). Observations with the MPFS and long-slit spectrograph were carried out in two spectral regions (“red” and “green”), and this allowed us to study the kinematics not only of the gaseous component but also of the stellar component.

NGC 7465. Let us consider the results of observations of the gaseous component of this galaxy. Figure 5c presents a large-scale line-of-sight velocity field in the $H\alpha$ line. It is obvious from the figure that the gas disk rotates, and the eastern side approaches us, while the western side recedes from us. In the central region of the galaxy ($r < 4''-5''$), a knee of isovels is noticeable. We will dwell on this feature below when discussing the MPFS data. At greater

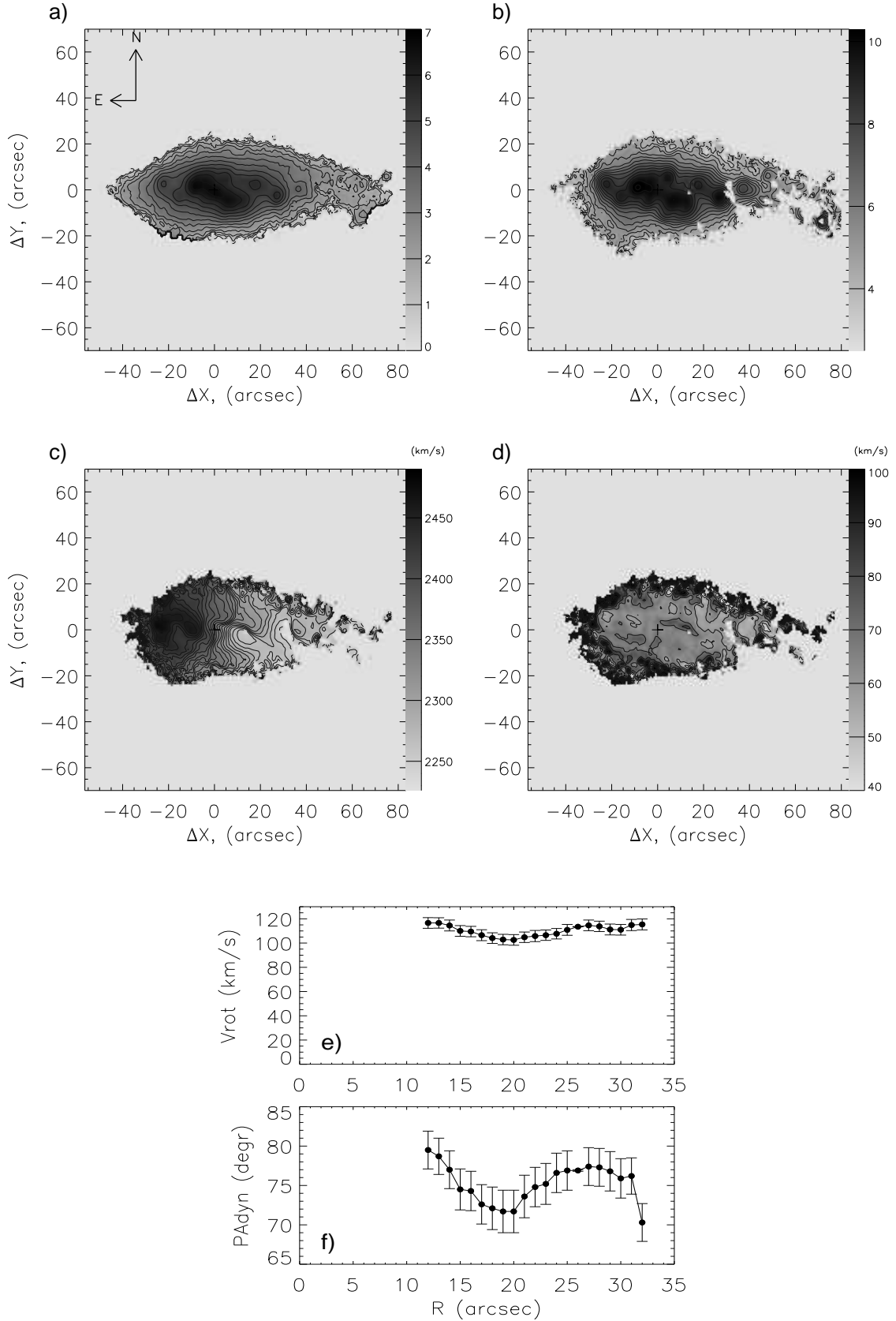


Figure 4: NGC 7463. Results from the IFP data: (a) — the brightness distribution in the narrow continuum near the H α line; (b) — the brightness distribution in the H α line; (c) — the line-of-sight velocity field in the H α line; (d) — the line-of-sight velocity dispersion field in the H α line. Results of the “tilted-ring” method: (e) — the rotation curve of the gas; (f) — $PA_{dyn}(R)$.

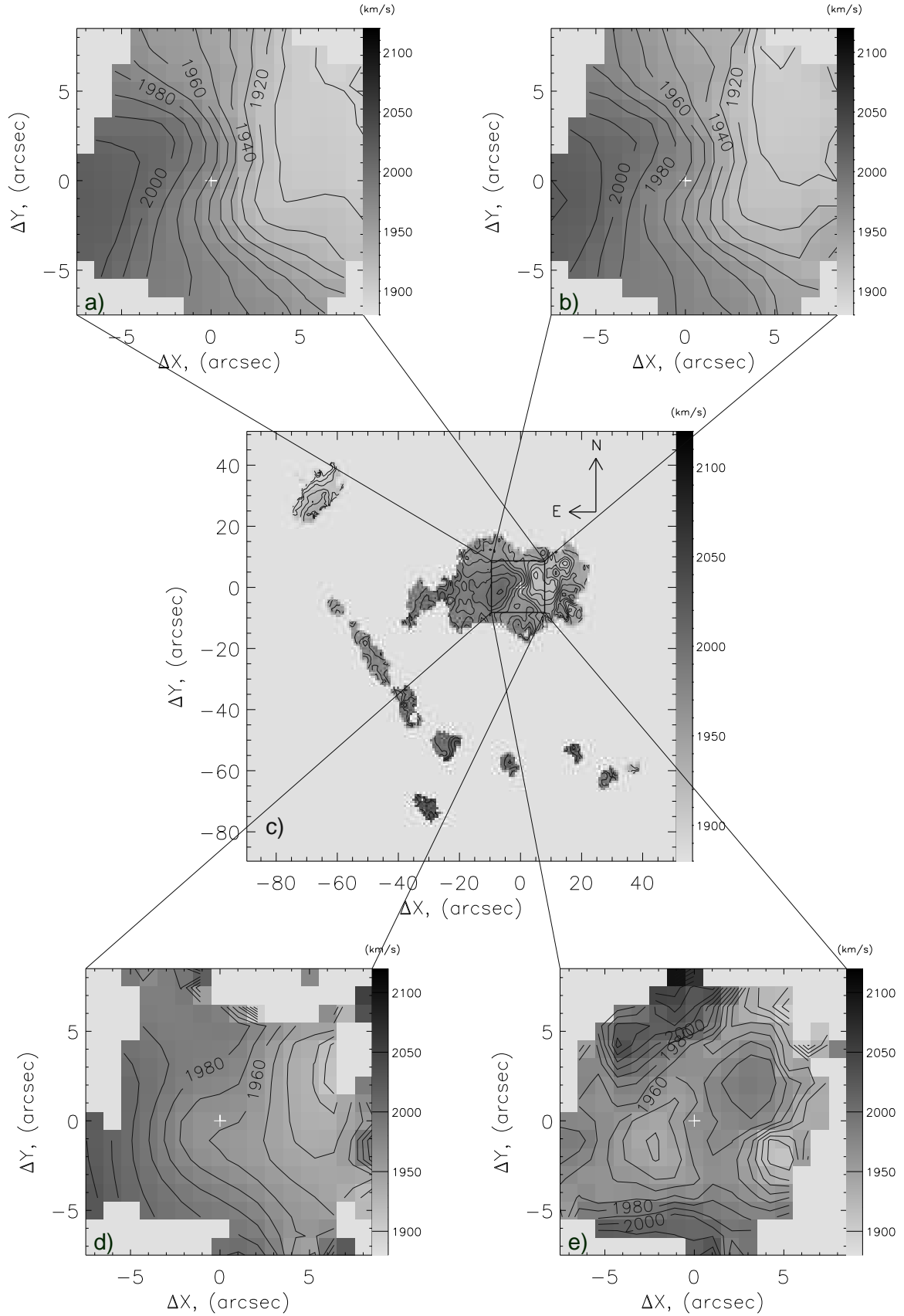


Figure 5: NGC 7465. Line-of-sight velocity fields of the ionized gas in the following lines: (a) — H α (MPFS); (b) — [NII] $\lambda 6584 \text{ \AA}$ (MPFS); (c) — H α (IFP); (d) — [OIII] $\lambda 5007 \text{ \AA}$ (MPFS). (e) — the line-of-sight velocity field of the stellar component (MPFS).

distances (up to $r \approx 20''-25''$), the shape of isovels corresponds to the rotation of a disk.

The analysis of the large-scale line-of-sight velocity field by the “tilted-ring” method has shown that the photometric and dynamic centers coincide and the heliocentric velocity of the system is 1963 km/s. Figure 6a shows a rotation curve of the ionized gas; the maximum rotation velocity is reached at the distance of $8''$ and is equal to 70 km/s, then it decreases, and in the region from $13''$ to $25''$ it changes little and is equal approximately to 40 km/s. The change of the position angle of the dynamic axis with the distance from the center is given in Fig. 6b. It is obvious from this figure that the dynamic axis turns smoothly with distance from the center, and the inclination of the disk to the plane of the sky changes too. Parameters of the model of circular rotation of the ionized gas turn out to be the following: at $r = 2''-3''$ $PA_{\text{dyn}} \approx 50^\circ$ and the inclination to the plane of the sky is $i_{\text{dyn}} \approx 50^\circ$; while in the region from $15''$ to $20''$ PA_{dyn} changes from 120° to 130° and $i_{\text{dyn}} \approx 60^\circ$.

For the central region of NGC 7465, velocity fields in all emission lines were constructed on the basis of the MPFS data. They turned out to be similar, therefore fields in the $H\alpha$, [NII] and [OIII] lines are given in Fig. 5a,b,d. In the circumnuclear region ($r \leq 3''$), a knee of isovels is observed, like according to the IFP data. As a whole the eastern part of the gas disk recedes from us, while the western part approaches us; the dynamic axis turns gradually with the increase of distance from the center from $PA_{\text{dyn}} \approx 70^\circ$ ($r = 2''$) to $PA_{\text{dyn}} \approx 110^\circ$ ($r = 8''$), and this coincides with data obtained with the IFP, within the errors limits.

As concerns bright condensations in $H\alpha$ that form the arc/semiring (see Fig. 5c), then (as we have mentioned when analyzing structures of this galaxy) the majority of them belong to different spiral arms (NE-, SE-, SW-arms). Their velocities most likely characterize line-of-sight velocities of gas in corresponding parts of spirals.

Line-of-sight velocity curves in emission lines (long-slit spectra) along major axes of the main body ($PA = 160^\circ$) and of the supposed polar ring ($PA = 45^\circ$) are similar to each other and agree well with the MPFS and IFP data. The coincidence of line-of-sight velocity values measured using three different spectral instruments, within the accuracy, indicates the reliability of our data.

Let us proceed to the consideration of kinematics of the stellar component. Figure 5e presents the velocity field of stars that was obtained from observations in the “green” range with MPFS. In the central region ($r \leq 4''-5''$), the shape of isovels is regular and typical for a rotating disk. The analysis of this field by the “tilted-ring” method has shown that $PA_{\text{dyn,st}} \approx 300^\circ$ and $i_{\text{dyn,st}} \approx 60^\circ$ and they are close to photometric parameters obtained by us in the previous section.

Let us consider the motion behavior of the stellar component of this galaxy according to the long-slit spectroscopy data. Figure 6c presents the line-of-sight velocity curve of stars along

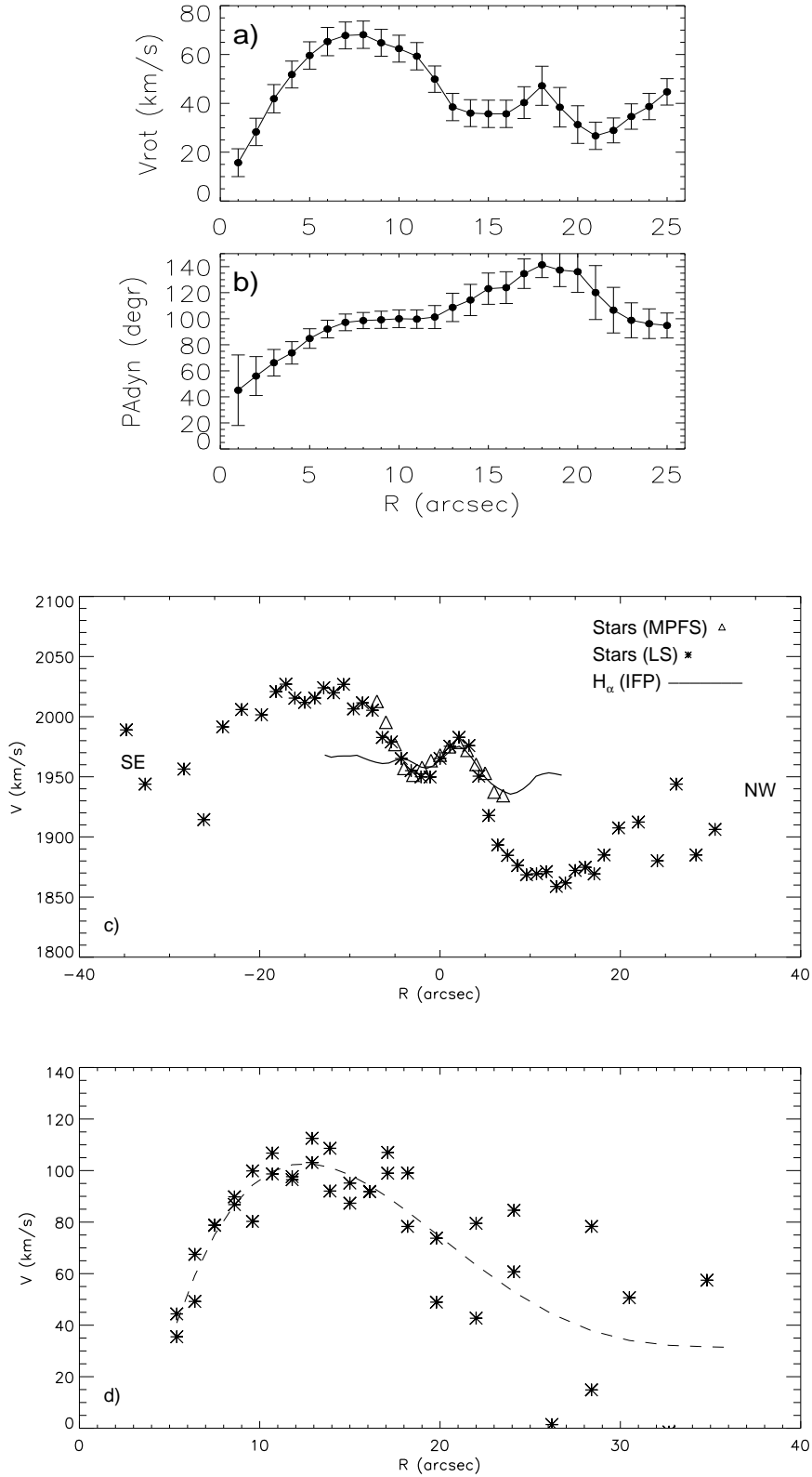


Figure 6: NGC 7465. Results of the “tilted-ring” method: (a) — the rotation curve of the ionized gas, (b) — $PA_{dyn}(R)$. (c) — line-of-sight velocity curves of stars (slit and MPFS) and of the ionized gas (IFP) along $PA = 160^\circ$; (d) — the rotation curve of stars (* — the observed values of the rotation velocity, dashed line — the average smooth rotation curve).

the major axis of the galaxy ($PA = 160^\circ$). Absorption lines are seen up to $30''$ from the center in this direction. Values of line-of-sight velocities of stars that were derived from observations with the long-slit spectrograph and MPFS coincide within the error limits. The change of the gradient direction to the opposite one is observed in the line-of-sight velocity curve of stars at $r \geq 6''$ (outside the MPFS's field of view) (Fig. 6c). This is probably connected with the rotation of the main stellar disk of the galaxy around its minor axis; the NW-side of the disk approaches us, while the SE-side recedes from us.

The comparison of the line-of-sight velocity curve of stars at $PA = 160^\circ$ with a cut of the line-of-sight velocity field in the $H\alpha$ line along the same direction (Fig. 6c) shows that line-of-sight velocities of stars and of the ionized gas differ considerably starting from the distance of $\approx 3'' - 4''$ from the center. This means that the rotation of these components in the given region occurs around different axes.

If we assume that the dynamic axis of the stellar disk in outer regions of the galaxy coincides with the photometric axis, then $PA_{\text{dyn,st}} \approx 160^\circ$ and the inclination of the stellar disk to the plane of the sky is $i_{\text{dyn,st}} \approx 50^\circ$. Under these assumptions we can construct the rotation curve of the stellar disk of the galaxy (Fig. 6d). The maximum rotation velocity is reached at the distance $r_{\text{max}} = 13''$ from the nucleus, and it is equal to ≈ 105 km/s.

On the basis of the study of the kinematics of stars we ascertained that in the central region of NGC 7465, a stellar disk-like structure is singled out, and its rotation axis is at a considerable angle ($\sim 140^\circ$) to the rotation axis of the main stellar disk.

Let us say a few words about line-of-sight velocity dispersions of the stellar and gas components. According to our data, the velocity dispersion of both stars and the ionized gas is small and does not considerably exceed determination errors. A small increase of the dispersion by 10–20 km/s is observed in the circumnuclear region ($r \leq 2''$) for both components.

NGC 7464. For this galaxy, line-of-sight velocity fields in the $H\alpha$ and $[\text{NII}]\lambda 6584\text{\AA}$ lines were constructed; they turned out to be similar, therefore the field in the $H\alpha$ line is given in Fig. 3c. Although the shape of isovels is not very smooth, the rotation of the galaxy with a small velocity is noticeable (the N-side recedes from us, and the S-side approaches us). A nucleus is clearly seen in the galaxy image in the continuum. The line-of-sight velocity at this point is ≈ 1765 km/s, and it is taken for the velocity of the system. It coincides with results of van Driel et al. (1992), but differs from neutral hydrogen data (Paturel et al., 2003; see Table 1) by 100 km/s. The asymmetry between N- and S-parts of the velocity field is observed: the S-part is more extended and is stretched in the direction of the spiral arm of the NGC 7465 galaxy. In addition, $PA_{\text{dyn}} = 240^\circ$ in the region $r \leq 5''$, while $PA_{\text{dyn}} = 185^\circ$ in more outer parts. Under the assumption of the circular rotation, we constructed the rotation curve (Fig. 3e) at the following parameters: $PA_{\text{dyn}} = 185^\circ$, $i_{\text{dyn}} = 40^\circ$, and $V_{\text{sys}} = 1765$ km/s. The maximum

value of the rotation velocity is reached at a distance of $9''$ and is equal to 40 km/s . Despite determination errors of these values, one can assert that NGC 7464 has the regular rotation.

The increase of the velocity dispersion from the N-edge of the galaxy to the S-edge by approximately 50 km/s is noticeable in the velocity dispersion map (Fig. 3d); this increase can be connected with the interaction with NGC 7465. Additional observations are necessary for the refinement of the velocity dispersion behavior.

NGC 7463. The line-of-sight velocity field of this galaxy is rather complex (Fig. 4c). It is known that in the bar region, noncircular motions should be observed, therefore we tried to analyze a part of the line-of-sight velocity field of NGC 7463 outside the bar ($12'' \leq r \leq 34''$) by the “tilted-ring” method. The model of the circular rotation of disk with the following parameters gave the best agreement with the observed field: positions of the photometric and dynamic centers coincide, the heliocentric velocity of the system is 2366 km/s , $\text{PA}_{\text{dyn}} \sim 75^\circ$, and under the assumption of the thin disk with $i_{\text{dyn}} = 62^\circ$. Figure 4e presents the corresponding rotation curve. In the region of $12'' \leq r \leq 34''$, the rotation velocity changes little and is equal to $\approx 115 \text{ km/s}$.

6 Discussion of results and conclusion

Photometric and spectral data obtained by us for the NGC 7465/64/63 triplet galaxies showed the interesting complex structure and kinematics in each of them. Let us note right away that we did not find the outer classical polar ring in NGC 7465 that was suspected by Whitmore et al. (1990). According to our data, the observed SE-arc (see images in $\text{H}\alpha$ (Fig. 1 right column on top)) consists of separate condensations belonging to different spiral arms. As it has turned out, the distribution and motion behavior of the ionized gas differ from corresponding data for the neutral hydrogen (Li and Seaquist, 1994); the ionized gas of this galaxy most likely forms its own detached system.

Moreover, such facts as the disturbed structure of NGC 7464, the stretching of its outer isophotes in the continuum and emission lines in the direction of NGC 7465, and the spiral arm extending from NGC 7465 to NGC 7464 led us the conclusion about the existence of the close connection between these galaxies. As a whole, photometric and spectral properties of NGC 7464 that were discovered by us (such as blue color indices; the presence of regular motions typical for disks) allowed us to relate it to the IrrI type.

In its turn, the whole set of our data for NGC 7463 shows that it is the barred spiral galaxy of the SBb-c type. However, the bend of its outer parts indicates that in the past, the close encounter of NGC 7463 with a galaxy went by occurred; it possibly was one of galaxies of the triplet or of the NGC 7448 group.

Let us discuss at greater length the results of the analysis of data for NGC 7465 that were obtained by us. In addition to the main stellar disk with the position angle of the major axis of 160° and with the inclination to the plane of the sky of $\sim 50^\circ$, the distinct inner (circumnuclear) stellar structure of the radius of $\sim 4''$ (0.56 kpc) with $\text{PA}_{\text{phot}} = 120^\circ$ was revealed in this galaxy. Photometric properties (the shape of isophotes in images in different spectral ranges, the approximation of the photometric cut along its major axis by the Sersic law with the index $n = 1 \pm 0.2$) and the stellar kinematics in the indicated region (the appearance of the velocity field of stars corresponds to the rotation of the disk with $\text{PA}_{\text{dyn,st}} = 300^\circ$ and $i_{\text{dyn,st}} \sim 60^\circ$) led us to the conclusion about the presence of the inner stellar disk almost “counter-rotating” relative to the main stellar disk.

On the basis of the large-scale brightness distribution in the $\text{H}\alpha$ line and of the complex behavior of isovels of the ionized gas in the region of radius of $25''$ ($\text{PA}_{\text{dyn,gas}}$ changes from $\approx 70^\circ$ at $r = 2''$ to $\text{PA}_{\text{dyn,gas}} \approx 120^\circ$ at $r = 20''$; $i_{\text{dyn,gas}} \sim 50^\circ$), we propose the presence of the warped gas disk; in the circumnuclear region ($r \leq 5''$), this gas disk is polar relative to the main stellar disk, and the estimation of an angle between planes of the main stellar disk and the gas disk (when calculating by its outer border) gives values of 45° and 83° . The observed circumnuclear dust lanes perpendicular to the major axis of the galaxy also speak in favor of the polarity of the gas disk (see, e.g., Sil’chenko and Afanasiev, 2004).

The origin of the observed structure of NGC 7465 that combines, at the minimum, three systems distinct by their properties (the inner and main stellar disks + the warped gas disk) is owed to the gravitational interaction with other galaxies. It seems unlikely to us that so complex structure was formed as a result of a single interaction. The circumnuclear stellar disk, most probably, could be formed as a result of the capture and disruption of a dwarf companion. The warped gas disk could arise in consequence of the accretion of the matter from a gas-rich galaxy onto NGC 7465 (Bournaud and Combes, 2003). Judging by our results, NGC 7464 could serve as such galaxy-companion.

The authors are grateful to the Large Telescope Program Committee for the allocation of the observational time at the 6-m telescope, to V.L. Afanasiev (SAO RAS) for the allocation of the Multi Pupil Fiber Spectrograph for our observations, A.V. Moiseev and S.N. Dodonov (SAO RAS) for the assistance in the carrying out of observations at the 6-m telescope, and separately to A.V. Moiseev for the allocation of data analysis codes and for valuable remarks in preparing the text of the paper. O.A. Merkulova is also grateful for the support within the event 1.4 of the Federal Target Program “Kadry” (contract no. 14.740.12.0852).

References

1. V.L. Afanasiev, S.N. Dodonov, V.L. Moiseev, *Stellar Dynamics: from Classic to Modern*. (Ed. Ossipkov L.P. and Nikiforov I.I., Saint Petersburg: St. Petersburg University, 2001),

2. V.L. Afanasiev and A.V. Moiseev, *Astron. Lett.* **31**, 194 (2005)
3. K.G. Begeman, *Astron. Astrophys.* **223**, 47 (1989)
4. F. Bournaud and F. Combes, *Astron. Astrophys.* **401**, 817 (2003)
5. C. Casini and J. Heidmann, *Astron. Astrophys. Suppl. Ser.* **34**, 91 (1978)
6. M.X. Fernandez et al., *Astron. J.* **139**, 2066 (2010)
7. P. Ferruit, A.S. Wilson, and J. Mulchaey, *Astrophys. J. Suppl. Ser.* **128**, 139 (2000)
8. R.I. Jedrzejewsky, *Mon. Not. R. Astr. Soc.* **226**, 747 (1987)
9. R.C. Kennicutt, *Ann. Rev. Astron. Astrophys.* **36**, 189 (1998)
10. A.U. Landolt, *Astron. J.* **88**, 439 (1983)
11. J.G. Li and E.R. Seaquist, *Astron. J.* **107**, 1953 (1994)
12. J.S. Mulchaey, A.S. Wilson, and Z. Tsvetanov, *Astron. J. Suppl. Ser.* **102**, 309 (1996)
13. A.V. Moiseev, *Bull. SAO* **54**, 74, (2002)
14. A.V. Moiseev and V.V. Mustsevoi, *Astron. Lett.* **26**, 565 (2000)
15. S.I. Neizvestnyi, *Izv. Spets. Astrofiz. Observ.* **17**, 26 (1983)
16. G. Paturel, G. Theureau, L. Bottinelli, et al., *Astron. Astrophys.* **412**, 57 (2003)
17. L.V. Shalyapina, et al., *Astronomy Letters* **33**, 520 (2007)
18. D.J. Schlegel, D.P. Finkbeiner, M. Davis, *Astrophys. J.* **500**, 525 (1998)
19. H.R. Schmitt and A.L. Kinney, *Astrophys. J. Suppl. Ser.* **128**, 479 (2000)
20. O.K. Sil'chenko and V.L. Afanasiev, *Astron. J.* **127**, 2641 (2004)
21. C.M. Springob, M.P. Haynes, P. Martha, et al., *Astrophys. J. Suppl. Ser.* **160**, 149 (2005)
22. B. Takase, *Astron. Soc. of Japan. Publications*, **32**, 605 (1980)
23. J. Tonry and M. Davis, *Astron. Astrophys.* **84**, 1511 (1979)
24. W. van Driel et al., *Astron. Astrophys.* **259**, 71 (1992)
25. B.C. Whitmore, R.A. Lucas, D.B. McElroy, et al., *Astron. J.* **100**, 1489 (1990)